Research
Green Chemical Engineering—Article

Laminar-to-Turbulence Transition Revealed Through a Reynolds Number Equivalence

Xiao Dong Chen

School of Chemical and Environmental Engineering, Soochow University, Suzhou 215123, China

A B S T R A C T

Flow transition from laminar to turbulent mode (and vice versa)—that is, the initiation of turbulence—is one of the most important research subjects in the history of engineering. Even for pipe flow, predicting the onset of turbulence requires sophisticated instrumentation and/or direct numerical simulation, based on observing the instantaneous flow structure formation and evolution. In this work, a local Reynolds number equivalence γ (ratio of local inertia effect to viscous effect) is seen to conform to the Universal Law of the Wall, where $\gamma = 1$ represents a quantitative balance between the abovementioned two effects. This coincides with the wall layer thickness ($y^+ = 1$, where y^+ is the dimensionless distance from the wall surface defined in the Universal Law of the Wall). It is found that the characteristic of how the local derivative of γ against the local velocity changes with increasing velocity determines the onset of turbulence. For pipe flow, $\gamma \approx 25$, and for plate flow, $\gamma \approx 151.5$. These findings suggest that a certain combination of γ and velocity (nonlinearity) can qualify the source of turbulence (i.e., generate turbulent energy). Similarly, a re-evaluation of the previous findings reveals that only the geometrically narrow domain can act locally as the source of turbulence, with the rest of the flow field largely being left for transporting and dissipating. This understanding will have an impact on the future large-scale modeling of turbulence.

© 2019 THE AUTHOR. Published by Elsevier LTD on behalf of Chinese Academy of Engineering and Higher Education Press Limited Company. This is an open access article under the CC BY-NC-ND license (http://creativecommons.org/licenses/by-nc-nd/4.0/).

1. Introduction

At present, predicting the onset of turbulence, even for pipe flow, requires sophisticated instrumentation and/or direct numerical simulation (DNS) [1–4], based on observations of the detailed instantaneous flow structure formation and evolution. However, all of this modern research is conducted around the classical critical Reynolds number (Re_c). Osborne Reynolds (1842–1912) carried out thorough laboratory investigations on the behavior of Newtonian fluids [5,6]. His most remarkable discovery was the identification of the two modes of flow phenomena: laminar flow and turbulent flow [5–7]. The experimental methodology and theory proposed by Reynolds to investigate the transition from one type of flow to another have inspired numerous researchers over generations. The transition between these two types of flow is marked by a dimensionless parameter attributed to Reynolds—that is, the Reynolds number (Re):

$$Re = \frac{\rho U d}{\mu} \tag{1}$$

where ρ is the fluid density (kg·m^{-3}), μ is the fluid viscosity (Pa·s), U is a characteristic velocity (m·s^{-1}), and d is a characteristic dimension of the object with which the fluid is in contact (m). In a pipe, d is the inner pipe diameter; however, if the fluid flows around the pipe outside (cross-flow), d becomes the outer diameter. This number has often been said to represent the ratio of the inertia forces to the viscous forces. As the most important parameter, the Re, together with other fluid-related dimensionless parameters, provides a powerful foundation for many friction, heat, and mass-transfer correlations in fluid flow-related problems. These are particularly useful in designing process equipment and process optimizations [7]. While appreciating the experiments carried out by Reynolds, it is notable that the diameter of the pipe was limited; hence, a large Re might be obtained mainly by changing the fluid viscosity and/or increasing the fluid velocity. Flow visualization took place in the central region of the pipe (the ink fluid was injected at the center location), so it would have been the result of the integrated or cumulative effect of turbulence generation along the pipe wall, transport, and dissipation. These three aspects would have been intertwined in the visualization in the experiments, and the Re should be viewed as a global parameter. In 1952, measurements in the proximity of the pipe wall showed a

very significant result: that using the friction velocity (u_r) and the product of the kinematic viscosity and the friction velocity (vu_r) to scale velocity and distance, respectively, away from the wall, a unique dimensionless velocity profile in the near-wall region was obtained. As calculated, based on the measurements, the rate of turbulence generation reaches a sharp maximum at the sub-layer thickness ($y^+ \approx 11.5$, where y^+ is the dimensionless distance from the wall surface defined in the Universal Law of the Wall (ULW)) [8]. From a rational perspective, the broad peak as shown may be better qualified as $y^+ \approx 11.5 \pm 5$. The commonly acknowledged divide between the laminar sub-layer and the buffer layer is marked at $y^+ = 5$ for a fully developed turbulent wall layer [8,9].

Micro-transient details of how a fluid transitions from being disturbed by localized perturbation into full-blown turbulence in a (long) pipe have only been captured very recently [1,2]. Sampling stations for local behaviors have been set up, facilitated by advanced computing power and modern experimental techniques. Experiments have been conducted below and above the well-known Re_c for pipe flow—that is, $Re_c = 2300$, where the subscript c represents critical.

In a small-diameter pipe in a laboratory setting, turbulence that is transient at low Re becomes sustained after a distinct Re_c; however, this phenomena was captured locally (unlike the general type of observation originally made by Reynolds) [1,2]. The critical point for transiting to sustained turbulence is decided when the local proliferation of puffs outweighs their decay. Experimentally artificial puffs were generated at precision to trigger turbulent behavior. Two timescales were captured (partly established through DNS) for the decay and spreading of the puffs. Plotting the Re dependence of the mean time until a second puff is nucleated and the turbulence fraction increases (declining with increasing Re), and the Re dependence of the mean time until the turbulence decays and the flow relaminarizes (increasing with increasing Re), creates a very sharp intersect at $Re_c = 2040 \pm 10$, marking the onset of laminar-to-sustained turbulence in pipe flow [1].

To explain this transition from laminar flow to turbulence, a bi-stability analysis with nonlinear propagation (advection) of turbulent fronts has been executed [2]. The interesting phenomena of destabilizing turbulence in pipe flow were subsequently studied using the same experimental strategies and DNS [3,4].

It is worth noting that most practical problems in this field, including airplane design, are simulated with semi-empirical turbulent models for turbulent kinetic energy and the Reynolds stresses. These models make computation more efficient. Although DNS is seen to be the ultimate way to directly generate images of turbulence, our knowledge about turbulence still mostly comes from intuitive prospects, whether reported or taught in classes.

In the present work, a dimensionless number is reported that is deduced intuitively from the concept of Re but applied to the local fluid flow. This dimensionless number is the ratio of the inertia effect to viscous effect, and its definition allows for an alternative analysis of the onset of turbulence, which has not previously been seen. Three classical cases in fluid mechanics are employed to show the effectiveness of the approach: the ULW, flow in a smooth circular pipe, and parallel flow on a smooth plate [9]. The analytical velocity profiles of these cases are well known [9–13], allowing derivations to be made to demonstrate the intended arguments precisely. This philosophy is in line with what Churchill [11] reported in his famous American Institute of Chemical Engineers Institute Lecture—that is, elucidating the fundamentals of transport phenomena without computational fluid dynamics.

Given this new number, beyond capturing the onset of turbulence, the author points to a significant possibility that turbulence (i.e., turbulent energy) originates from a very narrow domain(s) (defined by γ (ratio of local inertia effect to viscous effect) and velocity), leaving the rest of the flow field for transporting and dissipating turbulent energies. This perspective creates considerable scope for controlling turbulent flow and provides an idea for future improvements in turbulence-modeling effectiveness on large scales.

2. Main analyses

2.1. Defining the local ratio of inertia effect to viscous effect

To introduce the new dimensionless number, for simplicity, a semi-infinite Cartesian (x, y) parallel flow scheme, with one side bounded by a smooth flat solid wall (the smooth plate) is considered. Taking u as the local velocity in the x-direction (parallel to the plate), and recognizing that the predominant velocity gradient occurs in the y-direction, the prominent shear stress can be expressed as $\tau = -\mu \partial u / \partial y$. The no-slip condition is applied at the plate surface; hence, the scaling consideration leads to $\tau \approx -\mu(u_{ch} - 0)/\Delta_{ch}$. Here, Δ_{ch} is a characteristic distance corresponding to the representative velocity change of interest and u_{ch} is a characteristic velocity, where the subscript ch represents the characteristic value of the system. Taking the above to represent the viscous effects, a new dimensionless number is deduced: $\gamma = \rho u_{ch}^2/(\mu u_{ch}/\Delta_{ch})$. As $\Delta_{ch} \to 0$, the new local dimensionless number can be expressed locally:

$$\gamma = \frac{\rho u^2}{\mu |\partial u / \partial y|} \tag{2}$$

In Eq. (2), the absolute value is employed to avoid any confusion. Based on the derivation, it can be seen that this number is conceptually similar to the Re. It is argued that this number holds important physical meaning when interpreting fluid behavior at a finite point (x, y). If γ becomes very large, the viscous effect becomes negligible, and the fluid at that point should be able to maintain its pathway without changing direction. If the fluid flow becomes turbulent, the instantaneous velocity u in Eq. (2) may be replaced with the time-averaged local velocity $\bar{u}$, according to conventional wisdom. An appropriate value of γ must be attained in order to produce an eddy or eddies. On the other hand, the flow must be energetic enough to begin with, if turbulence can be sustained (i.e., u must be large). When the two effects are comparable, it should be found that $\gamma \approx 1$. It is envisaged that for different directions in a general flow domain, γ is directionally dependent. It is further noted that γ is in fact different from Re, because when the Re increases over a critical value, turbulence must occur. On the other hand, γ can vary from zero to infinity, even for laminar flows.

2.2. Conforming γ to the ULW

First, it is found that γ conforms to the ULW, thus demonstrating significant physical meaning. For a large Re, the wall-bounded turbulent flows exhibit boundary layers that fall within the dimensionless velocity distribution of an approximately universal nature. Many measurements have demonstrated the ULW [7–9]. Large-scale (industrial) turbulence modeling often takes advantage of the ULW to create a wall function in order to avoid detailed computations near the wall and thereby reduce the computing effort. In the ULW, the fluid boundary layer is divided into three regions: a (pure) viscous sub-layer (also called the wall layer), a buffer layer, and an overlap layer [9]. For the viscous sub-layer, $0 \leq y^+ < 5$ and $u^+ = y^+$, where $y^+ = y/\delta_v$. The wall layer thickness ($y^+ = 1$) is $\delta_v = v/u_r$. The friction velocity u_r is defined as $u_r = \sqrt{\bar{\tau}_w/\rho}$, where $\bar{\tau}_w$ is the time-averaged shear stress at the wall (N·m^{-2}). u^+ is defined as $u^+ = \bar{u}/u_r$.

This leads to the following:

$$\gamma = \left(\frac{y}{\delta_v}\right)^2 = (y^+)^2 \qquad (3)$$

Eq. (3) presents a significant finding that, in essence, when y is equal to the wall layer thickness, $\gamma = 1$, the inertia forces are comparable to the shear forces. It is also interesting to note that $y^+ = 5$ is the conventional divide for the viscous sub-layer and the buffer layer, at which $\gamma = 25$. $y^+ = 11.5$ may also be important, as this is where turbulence production has been reported to peak in the ULW. At this point, it is intuitive to think that there may be a critical γ that corresponds to the range marked by the above number moving from laminar to turbulence, provided that the fluid in this location has sufficient energy (or sufficiently high velocity). As mentioned above, in both laminar and turbulent flows, γ can vary from zero to infinity. Therefore, it is obvious that a single γ value cannot be a sole marker for generating turbulence.

2.3. Pipe flow

The strategy, then, is to seek the relationship between γ and changing velocity. As shown in Appendix A in the Supplementary data, γ can be obtained as a function of r/R (r is the radial coordinate and R is the radius of pipe) first for different Re(s), where Re is defined using the mean velocity u_m. Then, via the relationship between u and r in this classic case, γ can be further obtained as a function of u/u_m. Differentiating this u/u_m dependence function against u/u_m, for both the fully developed laminar and the fully developed turbulent regimes, yields a useful characteristic of γ varying with velocity. For laminar flow, it is the parabolic velocity profile; for turbulent flow, it is the 1/7th power velocity profile. It can be shown that at point $\gamma_{xx} \approx 25$ (corresponding to $y^+ = 5$), where the subscript xx indicates that the inertia effects in the x-direction interact with the shear effects applied in the x-direction as well, the crossover of the two derivatives against u/u_m yields $Re \approx 2083$. At this point, $u/u_m \approx 0.597$ (see Fig. S1 in the Supplementary data, which demonstrates the obtainment of this result). When the time-averaged velocity profile for turbulence is generalized to be of the 1/Nth order, where N is the power of the classic approximation of the time-averaged velocity distribution in turbulence regime (dimensionless), especially with $N = 11$, it can be shown that $Re = 2005.75$ is critical (see Appendix A in the Supplementary data). Here, the velocity at $\gamma_{xx} = 25$ and $\bar{u}/u_m = 0.650$ (see Fig. S2 in the Supplementary data). This analysis indicates that when $\gamma_{xx} = 25$, if the fluid flow at that location has sufficient power, turbulence occurs.

2.4. Plate flow

In contrast to the flow in a pipe, the flow parallel to and above a flat plate is at least two-dimensional. It is well known that the solution to a laminar velocity distribution in the plate boundary layer can be obtained accurately through similarity solution procedures [9]; that is, $\bar{u}/U_\infty = f(\eta)$, where η is the dimensionless transformation variable $\eta = y/\sqrt{\rho U_\infty/2\mu x}$ and U_∞ is the velocity of the bulk fluid. The laminar velocity profile can also be expressed in a parabolic format, while the turbulent profile can be expressed approximately as a 1/7th power format when scaled using the boundary layer thickness (see Appendix B in the Supplementary data). Once again, $d\gamma_{xx}/d(\bar{u}/U_\infty)$ can be obtained for both flow modes, respectively. The crossover is set at $Re_{x,c} = 5.5 \times 10^5$, which is the oft-mentioned Re_c for the onset of turbulence in plate flow. It is found that $\gamma_{xx} \approx 154.6$ ($y^+ \approx 12.4$) (see Appendix B in the Supplementary data). At this point, $\bar{u}/U_\infty = 0.441$. The obtainment of the critical parameter is shown in Fig. S3 in the Supplementary data.

In fact, the literature tends to suggest a range for the onset Re for turbulence of 10^5–10^6. The low estimate, $Re_{x,c} = 10^5$, yields $\gamma_{xx} = 89.24$ ($y^+ = 9.45$), for which $\bar{u}/U_\infty = 0.487$. This result actually aligns well with the critical condition for pipe flow.

2.5. Reversing back from turbulence to laminar flow

If the velocity profile is changed while the flow rate is kept the same in a smooth and straight pipe, it is interesting to see whether Re_c for the onset of turbulence changes or not. It is possible to pre-fix γ to be 25, and then see whether Re_c is influenced by altering the velocity profile. It is shown that when the law of 1/7th for turbulence is changed to the 1/20th law for turbulence, where the velocity profile becomes flatter, Re_c becomes 2485, in contrast to 2083 for the 1/7th law. In other words, it is possible to reverse the already turbulent situation "back" to the laminar situation if the velocity profile is somehow forced to be flatter in the gap of $Re = 2485$–2083. In general, when N becomes greater than 7, Re_c also increases. This result aligns well with the original work reported recently [3].

3. Further remarks

It has been successfully shown that the onset of turbulence can be interpreted through the introduction of γ, which is the ratio of local inertia effect to viscous effect. Based on the well-established velocity profiles, it is possible to evaluate the critical transition Re through the relationship of how the local derivative of γ against velocity changes with velocity. The sensitive region for flow transition is narrow, based on the analyses given in this work (see Figs. S1–S3 in the Supplementary data; beyond the crossover points, the change in the local derivative of γ against velocity (as well as that of γ) increases rapidly with increasing velocity, and no further crossover can be found). Increasing γ would dam the turbulence, even it was already generated. It is probable that only a very thin or narrow geometrical region (i.e., a line or a shell) is capable of sustaining turbulence generation. Upon a further analysis of previous results [1], albeit not elaborated in that study (see Fig. 5 in Ref. [1]), where the mean time of a puff from the wall before decaying or splitting as a function of Re in the pipe is shown, the occurrence of a very sharp critical phenomena is suggested. A lesser or greater Re than the Re_c has a much lower chance of producing sustained randomness (Fig. 1). A previous work [2] (see Fig. 3 in Ref. [2]) also shows that the level of turbulence reflected by the cross-stream velocity fluctuations v'/U does not actually increase much
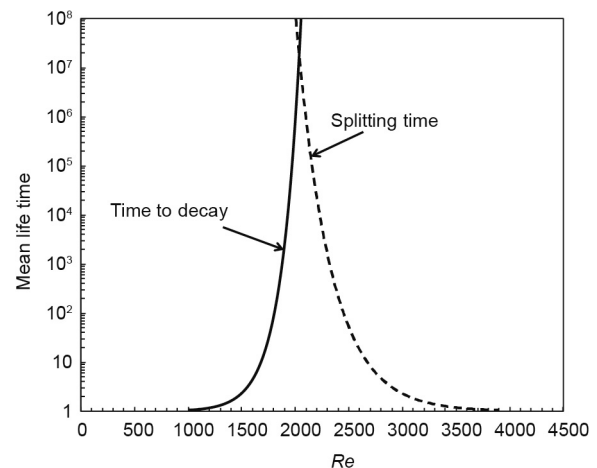

Fig. 1. Mean lifetime of a puff before decaying (solid line) or splitting (dashed line), plotted using the mean lifetime functions of the Re created previously [1].

with increasing *Re*, once past the Re_c. It is thus highly probable that the source of (strongest) turbulence is located in a narrow region (s); furthermore, if this were true, then the rest of the flow field would largely be left for the transportation and dissipation of turbulence energy. This perspective would have a profound influence on the modeling of turbulence.

In future studies, it will be helpful to visualize and compare the γ distribution for both laminar and turbulent regimes with the same flow arrangement and in the same device. Finally, it is emphasized again that despite the vast difference between the Re_c found for pipe flow and for plate flow, respectively, the current dimensionless parameters under critical conditions for the two cases are not that different.

Acknowledgements

Nomenclature

d	characteristic dimension of the object (m)
Re	Reynolds number (dimensionless)
U	characteristic velocity (m·s^{-1})
$u, \bar{u}$	local velocity and time-averaged local velocity, respectively (m·s^{-1})
U_∞	velocity of the bulk fluid in plate flow (m·s^{-1})
u_m	mean velocity (m·s^{-1})
u_r	friction velocity (m·s^{-1}) as defined in the ULW [8–12]
v	kinematic viscosity (m^2·s^{-1})
r	the radial coordinate (m)
R	the radius of pipe (m)
N	the power of the classic approximation of the time-averaged velocity distribution in turbulence regime (dimensionless)
u_{ch}	a characteristic velocity (m·s^{-1})
x	*x*-coordinate in the Cartesian system
y	*y*-coordinate in the Cartesian system
y^+	dimensionless distance from the wall surface defined in the ULW
δ_v	wall layer thickness (m) [8,13]
Δ_c	characteristic distance corresponding to the representative velocity change (m)
γ	ratio of local inertia effect to viscous effect (dimensionless)
η	dimensionless transformation variable in the classic similarity solution of plate flow
μ	fluid viscosity (Pa·s)
ρ	fluid density (kg·m^{-3})
$\tau, \bar{\tau}$	shear stress and time-averaged shear stress, respectively (Pa)

Appendices A and B. Supplementary data

Supplementary data to this article can be found online at https://doi.org/10.1016/j.eng.2018.09.013.

References

[1] Avila K, Moxey D, de Lozar A, Avila M, Barkley D, Hof B. The onset of turbulence in pipe flow. Science 2011;333(6039):192–6.

[2] Barkley D, Song B, Mukund V, Lemoult G, Avila M, Hof B. The rise of fully turbulent flow. Nature 2015;526(7574):550–3.

[3] Hof B, de Lozar A, Avila M, Tu X, Schneider TM. Eliminating turbulence in spatially intermittent flows. Science 2010;327(5972):1491–4.

[4] Kühnen J, Song B, Scarselli D, Budanur NB, Ried M, Willis AP, et al. Destabilizing turbulence in pipe flow. Nat Phys 2018;14(4):386–90.

[5] Reynolds O. An experimental investigation of the circumstances which determine whether the motion of water shall be direct or sinuous, and of the law of resistance in parallel channels. Philos Trans R Soc Lond 1883;174: 935–82.

[6] Tokaty GA. A history and philosophy of fluid mechanics. New York: Dover; 1971.

[7] Bird RB, Stewart WE, Lightfoot EN. Transport phenomena. 2nd ed. New York: John Wiley & Sons; 2002.

[8] Laufer J. The structure of turbulence in fully developed pipe flow. NACA technical report. United States: National Bureau of Standards; 1953 Jun. Report No.: NACA-TN-2954.

[9] Schlichting H, Gersten K. Boundary-layer theory. 8th ed. Berlin: Springer; 2003.

[10] Churchill SW. Progress in the thermal sciences: AIChE Institute Lecture. AIChE J 2000;46(9):1704–22.

[11] Nikuradse J. Gesetzmassigkeiten der turbulenten stromung in glatten rohren. Berlin: VDI Verlag; 1932. German.

[12] Pai SI. On turbulent flow in circular pipe. J Franklin Inst 1953;256(4): 337–52.

[13] Çengel YA, Cimbala JM. Fluid mechanics—fundamentals and applications. 2nd ed. New York: McGraw-Hill Higher Education; 2006.